Coupling the Stochastic Particle-resolved Aerosol Model PartMC-MOSAIC with WRF

Jeffrey H Curtis
Department of Atmospheric Sciences
University of Illinois at Urbana-Champaign
`jcurtis2@illinois.edu`

Nicole Riemer
Department of Atmospheric Sciences
University of Illinois at Urbana-Champaign
`nriemer@illinois.edu`

Matthew West
Department of Mechanical Science and Engineering
University of Illinois at Urbana-Champaign
`mwest@illinois.edu`

PartMC Beyond the Box

The chemical reactivity, cloud condensation nuclei activity and radiative properties of black-carbon-containing particles depend crucially on the aerosol mixing state. The recently developed particle-resolved aerosol box model PartMC-MOSAIC (Riemer et al., 2009) has allowed unique insight into the evolution of aerosol mixing state. Here we show how we take PartMC-MOSAIC to the next level by coupling it with the Weather Research and Forecast model (WRF). This creates a model that not only resolves per-particle size and composition but also the spatial structure of the atmosphere. The coupled model with detailed mixing state allows for high resolution case studies and the ability to benchmark more approximate aerosol models.

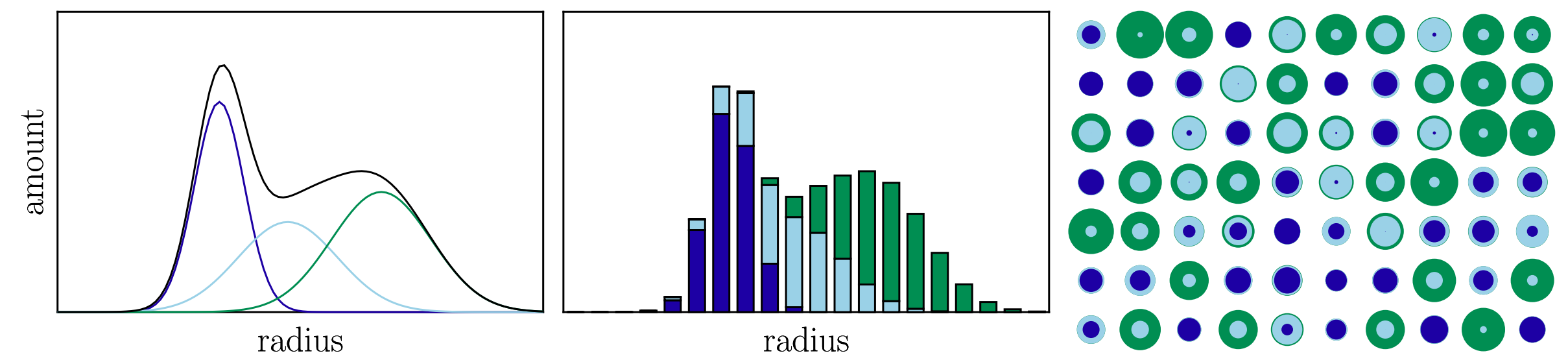

Figure 1: Left: Modal aerosol models represent the aerosol size distribution as a sum of modes. Center: Sectional models store the number or mass of aerosol per bin. Right: By contrast, a particle-resolved model such as PartMC can track complex internal mixing states.

Model Description

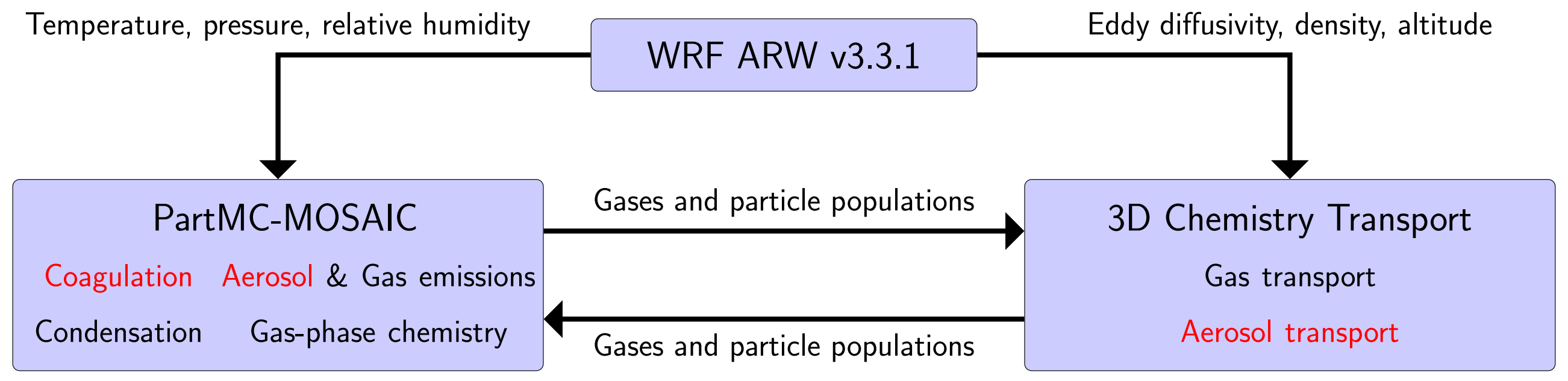
Temperature, pressure, relative humidity
WRF ARW v3.3.1
Eddy diffusivity, density, altitude
PartMC-MOSAIC
Coagulation Aerosol & Gas emissions
Condensation Gas-phase chemistry
Gases and particle populations
Gases and particle populations
3D Chemistry Transport
Gas transport
Aerosol transport

Figure 2: Module diagram of the coupled WRF-PartMC-MOSAIC model with computationally efficient stochastic model processes denoted in red. WRF provides meteorological information for both aerosol and gas phase chemistry and determines the transport of chemical species and aerosols.

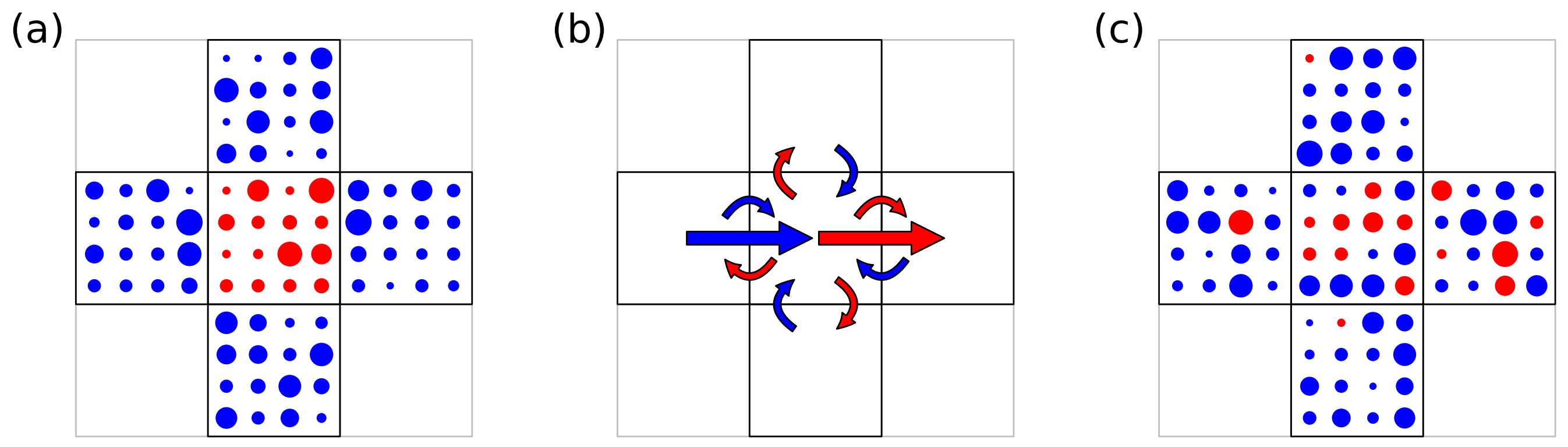

Figure 3: (a) Particle populations at time t before the transport event (b) Schematic of the 2D transport due to advection, here assumed as a positive u velocity and transport due to turbulent diffusion, and (c) particle populations at time $t + \Delta t$ after transport with advection probabilities of $\frac{1}{4}$ and diffusion of $\frac{1}{16}$.

Verification of Stochastic Particle Transport

To verify the algorithm implemented for stochastic particle transport, an idealized 2-D advection-diffusion test case, where gas initial concentrations and emission rates and aerosol initial concentrations and emission rates have a fixed ratio R to each other. This allows us to compare the stochastic particle transport solution to the finite volume solution of the gas concentration. As the number of computational particles $N_{\rm p}$ for a simulation increases, the solution is expected to converge to the finite volume solution as shown in Figure 4.

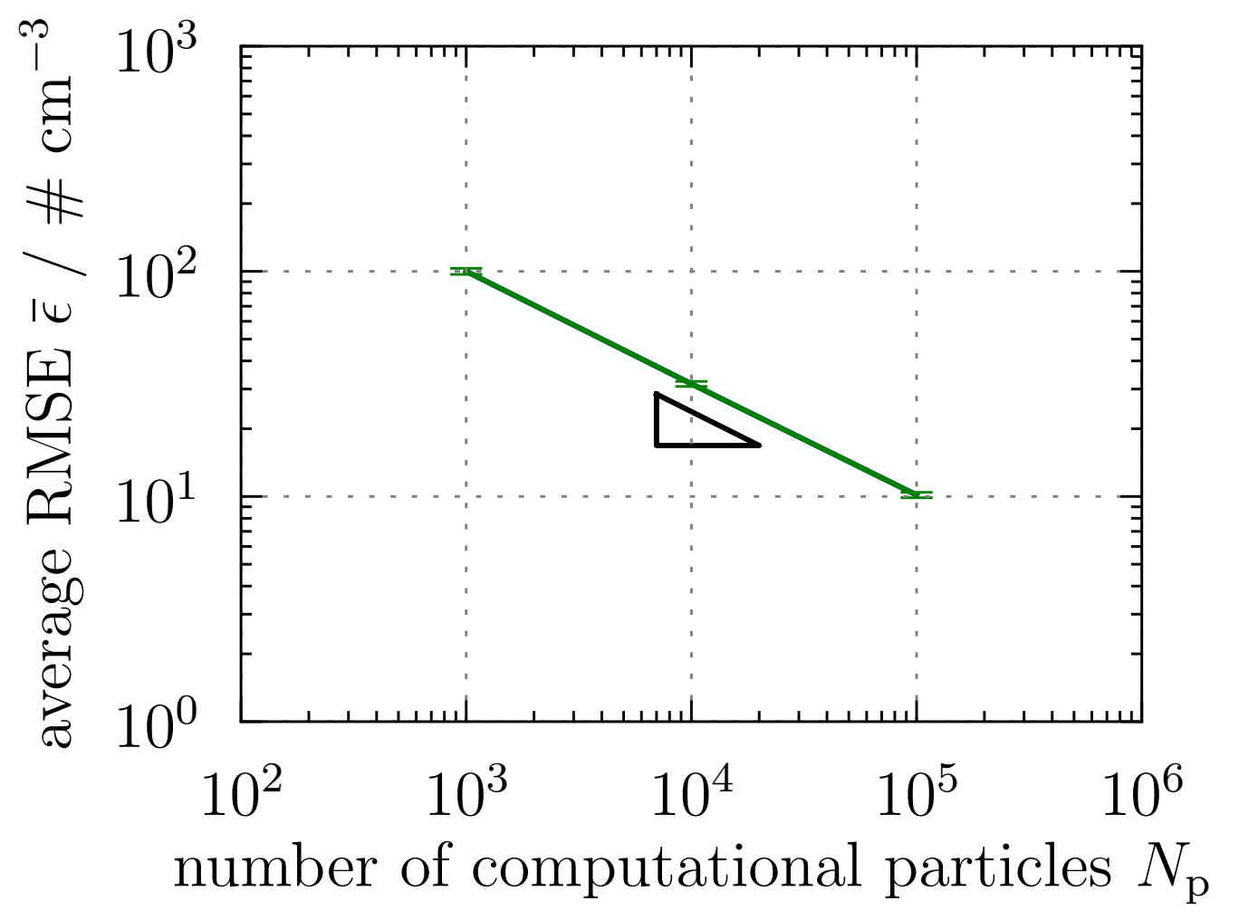

$N_{i,j}$: number concentration of grid cell i,j

$\Phi_{i,j}$: gas concentration of grid cell i,j

Root mean square error:

$$\epsilon_k = \sqrt{\frac{1}{(n_{\rm x})(n_{\rm y})}\sum_{i=1}^{n_{\rm x}}\sum_{j=1}^{n_{\rm y}}\left(N_{i,j}^k - R\Phi_{i,j}\right)^2}$$

Average RMSE error:

$$\bar{\epsilon} = \frac{1}{n_{\rm run}}\sum_{k=1}^{n_{\rm run}}\epsilon_k$$

Figure 4: The average root mean square error $\bar{\epsilon}$ of the number concentration. Ensemble size $n_{\rm run}$ of 30. Error bars denote 95% confidence interval. The expected slope is $-\frac{1}{2}$ for particle methods as convergence scales with $\sqrt{N_{\rm p}}$.

Idealized 3-Dimensional Plume Scenario

An idealized urban plume scenario was simulated for a 6 hour period. Black carbon containing particles were emitted at a constant rate from one particular grid cell at the surface. Particles were transported by advection with a probability of 7.5%, equal to a mean wind speed of 5 m s^{-1}, and by turbulent diffusion in the horizontal and vertical directions with a probability of 1%. The domain was $n_{\rm x} = 40$, $n_y = 30$, and $n_z = 60$. We initialized the simulation with 10 000 computational particles per grid cell.

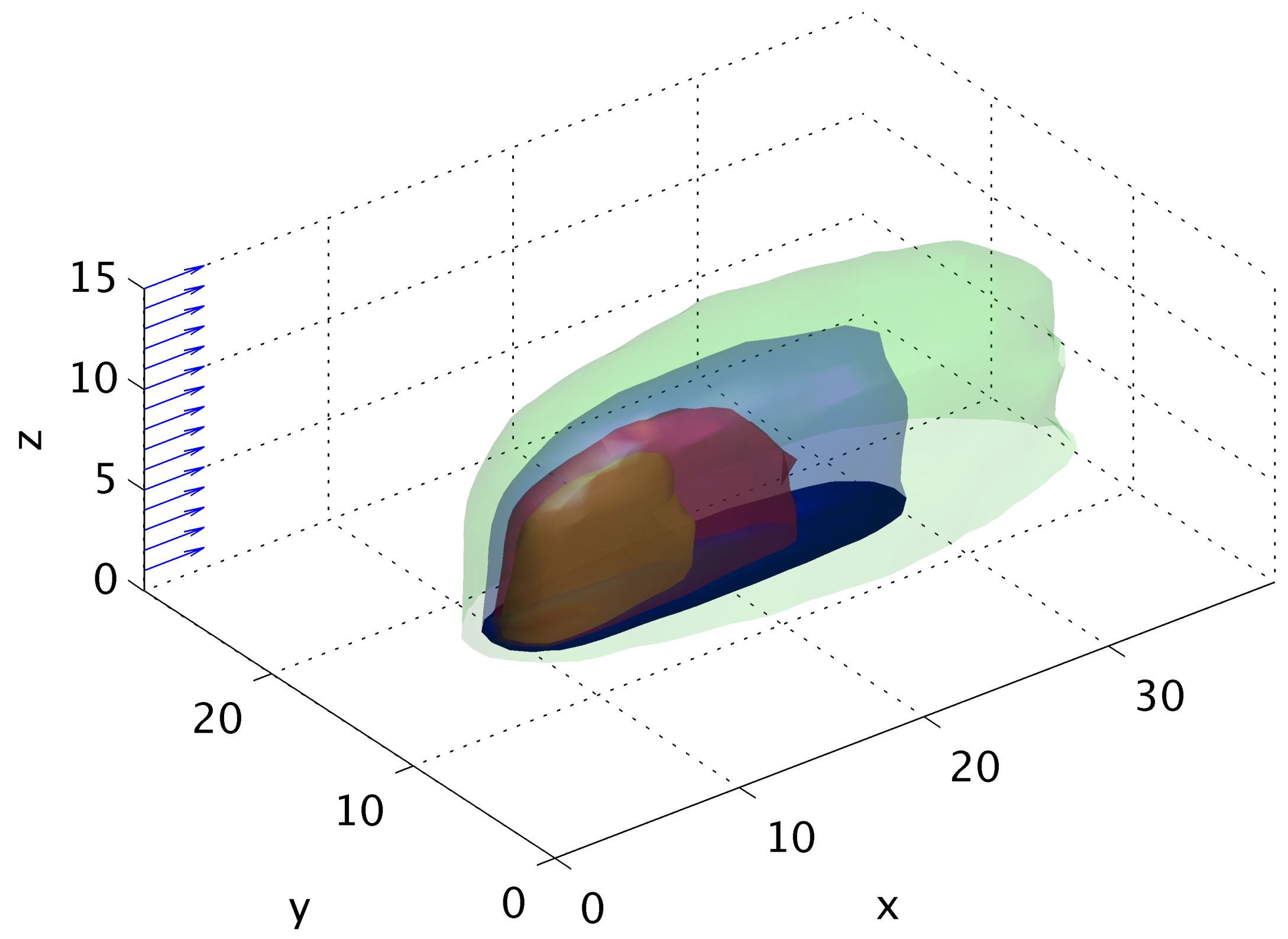

Figure 5: Isosurfaces of black carbon mass concentrations for the plume at $t = 6$ h.

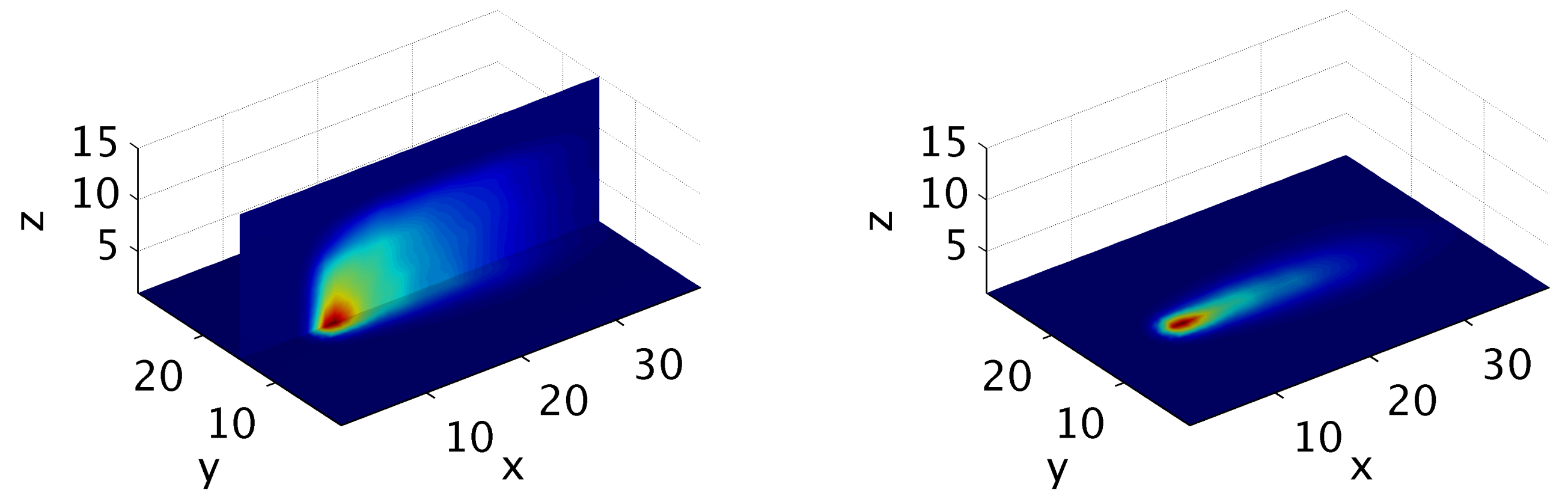

Figure 6: (Left) Cross section of black carbon mass concentration of the X-Z plane along the centerline of the plume at $t = 6$ h. (Right) Cross section of black carbon mass concentration along the X-Y plane of the lowest model layer at $t = 6$ h.

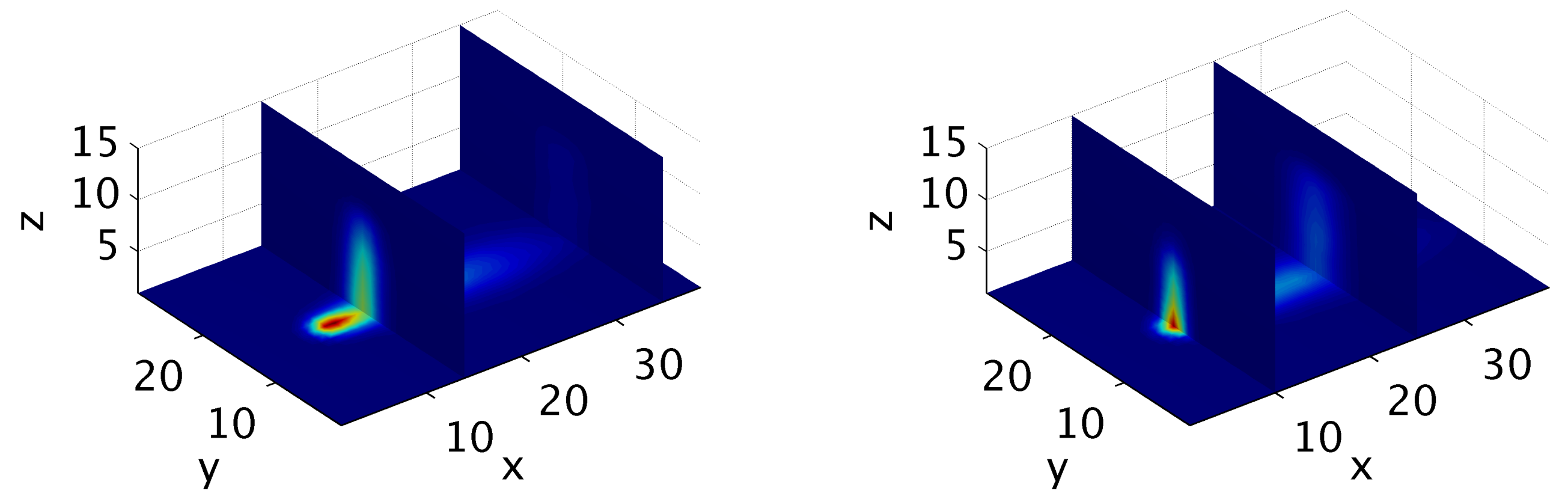

Figure 7: Y-Z cross sections of black carbon mass concentration at different distances downwind from the emission source at $t = 6$ h.

Computational Demands

Particle-resolved modeling has high computational demands in comparison to the more approximate aerosol representations shown in Figure 1.

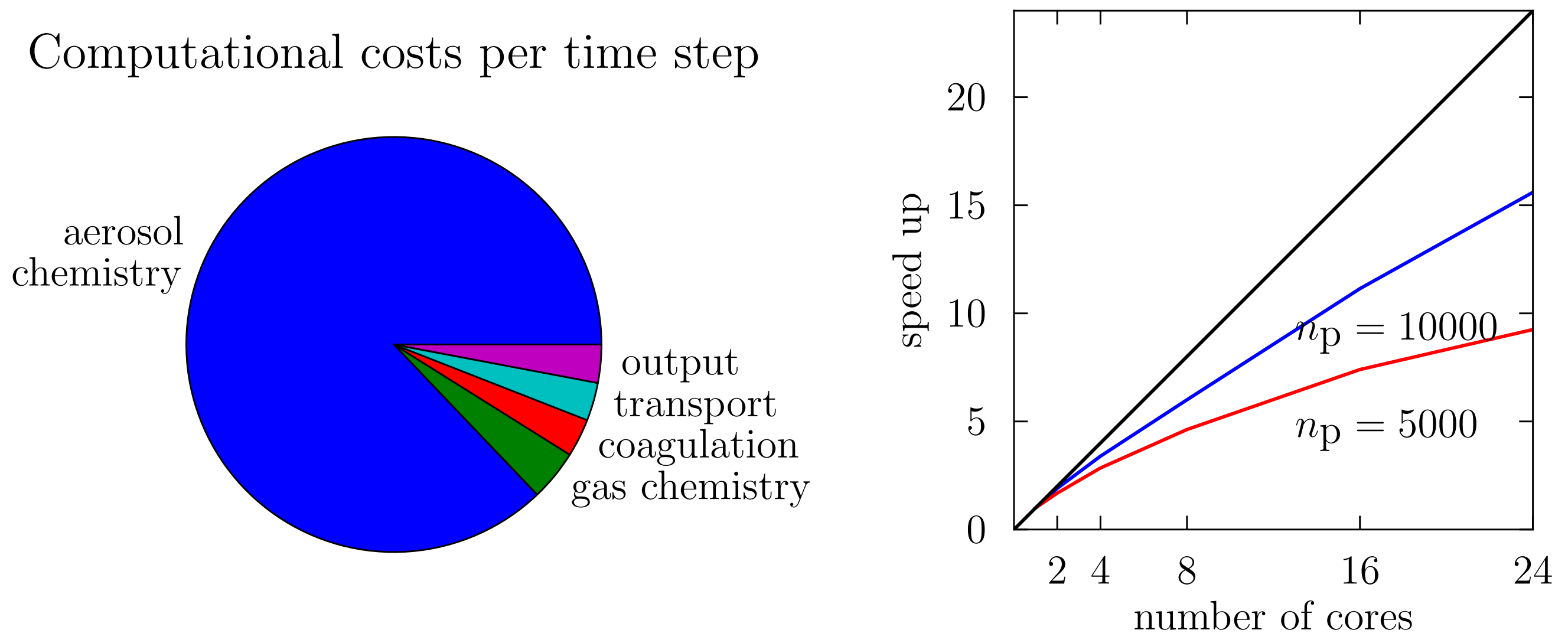

Figure 8: (Left) The proportion of computational time spent on major processes within the 3D model. (Right) Speedup versus number of cores. Speedup becomes more pronounced with greater number of computational particles as chemistry and coagulation dominate over processes that require communication.

Conclusions

- We have successfully implemented a framework for 3D stochastic transport of aerosols where the stochastic solution converges to the finite volume solution.
- By coupling PartMC-MOSAIC and WRF, we created a model that is not only capable of resolving per-particle size and composition, but also resolves the spatial distribution of particles.